Single-Atom Metal Supported at Two-Dimensional MoS_2

Subjects: Environmental Sciences

Contributor: Jiahao Wang , Xiaorong Gan , Tianhao Zhu , Yanhui Ao , Peifang Wang

Due to increasing concerns about global warming and energy crisis, intensive efforts have been made to explore renewable and clean energy sources. Single-atom metals and two-dimensional (2D) nanomaterials have attracted extensive attention in the fields of energy and environment because of their unique electronic structures and excellent properties.

single-atom metal two-dimensional nanomaterials water splitting CO2 reduction catalysis DFT

1. Introduction

Due to the contamination and global warming problems, it is necessary to search for alternative environmentally friendly energy sources and decrease the concentration of CO_2 in the atmosphere [1][2][3]. The utilization of nonprecious metal electrocatalysts for water splitting and CO_2 fixation for producing high-value-added fuels or chemicals may be the ultimate solution for sustainable and clean hydrogen energy, tackling the challenges posed by rising CO_2 levels, and realizing a closed carbon cycle [4]. Proper electrocatalysts are extremely useful for improving the reaction rate of CO_2 conversion to its reduced oxidation states, CO and formate/formic acid. From the perspective of reactivity, CO_2 is chemically inert, and the initial bond energy of C=O is 806 kJ mol^{-1}, so the conversion of CO_2 into various products is a difficult problem in thermodynamics. Therefore, to make CO_2 conversion happen at a reasonable rate, the potential energy necessarily needs to be much greater than the thermodynamic values. Once the reaction is started, CO_2 can be converted into a mixture of products, mainly including carbon monoxide (CO), methane (CH_4), ethylene (CH_2CH_2), methanol (CH_3OH), ethanol (C_2H_5OH) formic acid (HCOOH), and acetate (CH_3COOH). In addition, hydrogen is a by-product produced at a potential close to the potential for CO_2 reduction [5][6][7][8][9]. However, the electrocatalysts for the CO_2 reduction reaction (CO_2RR) and water splitting face some problems, such as low product selectivity, poor faradaic efficiency (FE), and/or hard experimental conditions (in acidic media) [10][11]. In particular, the catalytic activity and selectivity of non-precious metal catalysts are generally much lower than those of noble metal catalysts [12]. The activity of catalysts is not only related to the composition and structure but also to the dimension or size. The most direct effect of the decrease in dimension or size is the change in the number of active sites. Compared to conventional nanoparticles, single-atom catalysts (SACs) have the advantages of unique electronic structure, strong metal-support interactions (SMSIs), and plenty of accessible active sites and thus can significantly improve catalytic activity and selectivity [13][14][15]. Therefore, SACs have shown prominent activity in various electrochemistry processes, including CO_2RR [16][17], oxygen evolution reaction (OER) [18][19], and hydrogen evolution reaction (HER) [20][21]. However, since the surface energy increases with the decrease in particle size, the single atoms tend to aggregate into clusters or nanoparticles [22][23], which leads to degraded functions. Hence, it is indispensable to anchor the isolated atoms onto the appropriate supports to build stable configurations with atomic distribution [24][25]. On one hand, proper supports can serve as stabilizing functions via metal-support interactions [26]. The strong metal–support interactions can effectively tune the electronic structure of SACs to improve the electrocatalytic activity and selectivity [27][28][29]. Two-dimensional materials are recognized as ideal supports for SACs and as preferable alternatives for catalysts due to their unique electronic properties, high specific surface area, and substantial number of active sites [30][31][32][33]. For example, Mn supported on 2D VTe_2 exhibits excellent catalytic performance for both HER and OER [34]. Recent advances have demonstrated that 2D materials can improve the performance of SACs and the inhomogeneity of active sites [35][36][37].

Two-dimensional molybdenum disulfide (MoS_2), as the representative of transition metal dichalcogenides (TMDCs), has attracted much attention for HER, OER, and CO_2RR due to its unique structure and easy functionalization [38][39]. In addition, owing to the high earth abundance, low price, and high HER catalytic activity, 2D MoS_2 is regarded as a promising alternative for noble metals for water splitting [40]. In addition to water splitting, 2D MoS_2 has a great potential application in CO_2RR because Mo-exposed edges can enhance the chemisorption of the reactants and thus improve the electrochemical catalysis with a low overpotential of CO_2RR (about ~54 mV) and high selectivity (the reduction product is only CO) [39][41]. However, the electrocatalytic performance of pristine 2D MoS_2 is still not satisfactory mainly due to the lack of active sites at its basal plane and low conductivity. For example, MoS_2 edges show poor oxygen evolution reaction (OER) activity [42], and the pristine basal plane of MoS_2 is inert to the electrochemical reduction of CO_2 [43]. Therefore, the successful combination of 2D MoS_2 and single-atom metal can not only minimize the drawbacks and maximize the advantages of the individual components; more importantly, in addition to the desired performances, some novel functions may be generated for enhancing electrocatalytic CO_2RR and overall water splitting.

Recently, single-atom metal/2D MoS_2 hybrid nanomaterials have been booming in heterogeneous electrocatalysis, due to well-defined located metal centers, unique metal–support interaction, and identical coordination environment. However, there have been only a few studies on the systematic summarization of the nanomaterials for electrocatalytic CO_2RR and overall water splitting.

2. Synthesis Methods of Single-Atom Metal/2D MoS_2 Hybrid Nanomaterials

The catalytic performances are determined by concrete improvements of synthetic methodologies [44]. The most widely employed approaches for SACs are pyrolysis, atomic layer deposition (ALD) method, physical vapor deposition (PVD), wet-chemistry strategy, and electronic deposition [45][46][47]. However, it is still hard to manipulate atoms in a highly accurate way for the control synthesis of theoretically designed SACs due to ultrahigh surface free energy. The synthesis methodologies for 2D MoS_2 can be divided into two categories: top-down and bottom-up methods. The former mainly includes chemical vapor deposition (CVD) and solvothermal or hydrothermal methods [48][49][50][51][52]; the latter includes mechanical exfoliation, chemical or electrochemical exfoliation methods, and liquid-phase exfoliation [53]. However, the number of successful cases for single-atom metal/2D MoS_2 hybrid nanomaterials is still limited compared to the synthesis methods for single-atom metal modified 3D supports, SACs preparation, and/or 2D materials. The methods for single-atom metal/2D MoS_2 hybrid nanomaterials are derived from the approaches for SAC@3D supports, such as pyrolysis and coprecipitation. Considering that the common synthetic methods of SACs or 2D materials have been discussed in depth in previous reviews, this research focuses on some novel methods for single-atom metal/2D MoS_2 hybrid nanomaterials, including the one-pot chemical method, the electrochemical process, and the polyoxometalate template-based synthetic strategy (**Figure 1**).

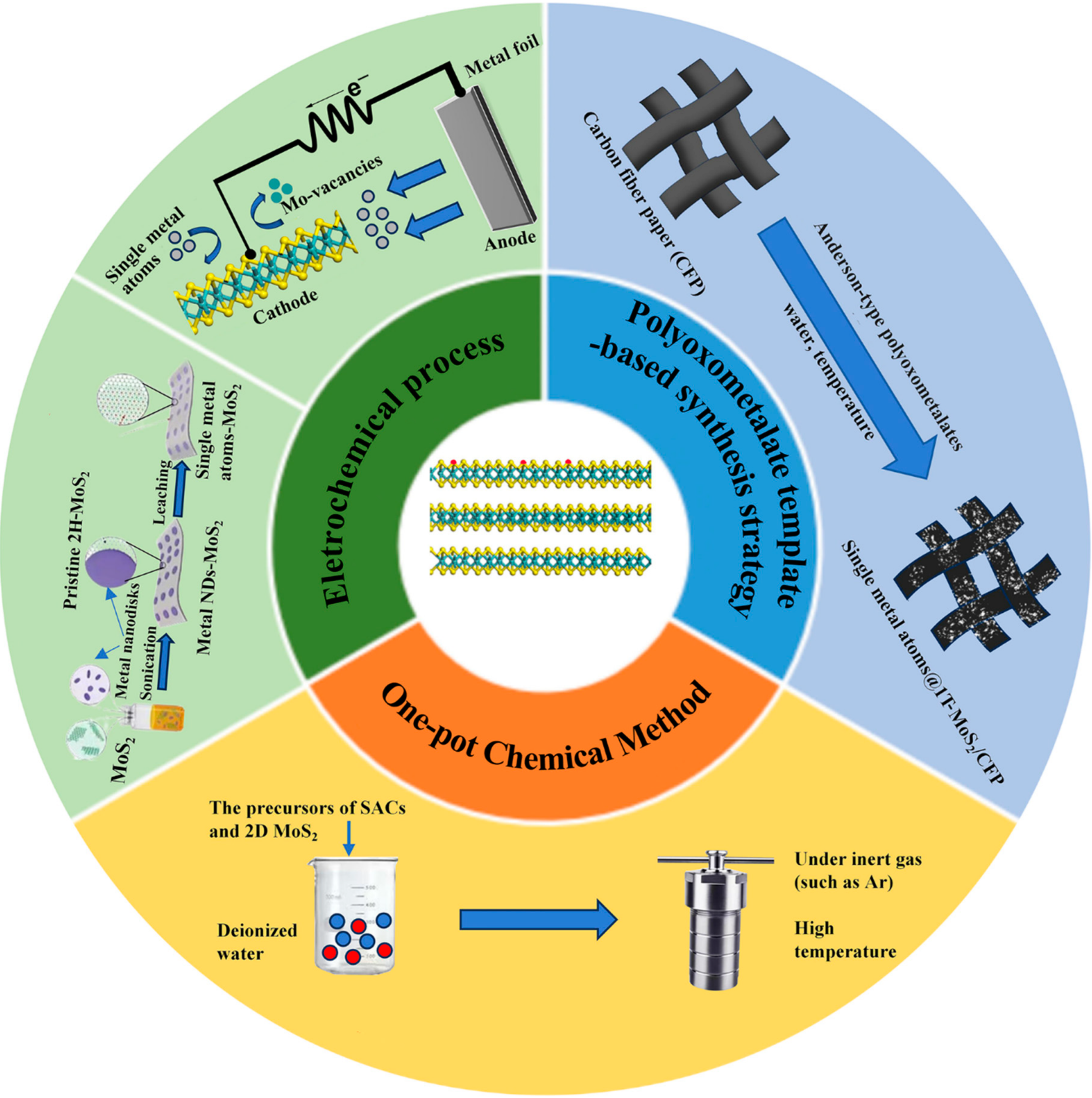

Figure 1. Several common synthesis methods of single-atom metal/2D MoS_2 hybrid nanomaterials.

2.1. One-Pot Chemical Method

The principle of this method is directly to mix the precursors of SACs and 2D MoS_2 for the following reactions under inert gas (e.g., Ar). The typical processes are described as follows: firstly, all precursors (e.g., $(NH_4)_6Mo_7O_{24}·_4H_2O$, H_2PtCl_6, and CS_2) are dissolved in a certain amount of deionized water to form a homogeneous solution [20]; then, the resulting solution is transferred to a Teflon-lined stainless autoclave under Ar and maintained at a high temperature for a certain reaction time.

The one-pot method has the advantages of simple operation and saving synthetic costs. In addition, the catalysts prepared by this method can have sulfur vacancies and the doping features of metal atoms at the same time [54]. Until now, Cu@1T-MoS_2, Ni@1T-MoS_2, Fe@1T-MoS_2, and Co@1T-MoS_2 have been easily prepared through this method [55].

2.2. Electrochemical Process

The electrochemical process is used to synthesize SAC-modified 2D MoS_2 via electrochemical etching of big-size metal precursor. Taking the single-atom cobalt (Co) array modified 2D MoS_2 as an example, firstly 2D MoS_2 and Co nanodisks (NDs) are synthesized using standard solvothermal procedures and standard air-free procedures, respectively. Then, the combination of Co NDs and 2D MoS_2 is realized via an assembly process. Finally, single-atom Co array covalently bound onto distorted 1T-MoS_2 nanosheets (denoted as SA Co-D 1T-MoS_2) via Co-S bonds can be synthesized through electrochemical cyclic voltammetry (CV) leaching of Co nanodisks (NDs). In addition to electrochemical CV leaching, the electrochemical deposition can be used to synthesize the nanocomposites of SACs modified 2D MoS_2, such as Pt, Cu, Sn, and Pd anchored on the 2D MoS_2, because these single metal atoms (from metal ions in the electrolyte solution) can be introduced onto the MoS_2 monolayer driven by applying the bias potential [56].

2.3. Polyoxometalate Template-Based Synthetic Strategy

Highly purified and stable metallic 1T-MoS_2 can be obtained via a hydrothermal method which introduces organic sulfur sources into $(NH_4)_6Mo_7O_{24}·4H_2O$ (denoted as Mo_7). Here, Mo_7 is a precursor that is a butterfly-shaped metal oxide cluster, and it belongs to the β-isomer of Anderson-type polyoxometalates (POMs). In addition, its unique structure makes it possible to tune the chemical environment of 1T-MoS_2 with various metal atoms. Using Anderson-type polyoxometalates ($[XH_6Mo_6O_{24}]^{n-}$) as precursors, atomically designing metal doping sites onto metallic 1T-MoS_2 can be achieved. $[XH_6Mo_6O_{24}]^{n-}$ is denoted as XMo_6 (X = Fe^{III}, Co^{III}, n = 3; X = Ni^{II}, n = 4) [53].

3. Applications of Single-Atom Metal/2D MoS_2 Hybrid Nanomaterials

3.1. Electrochemical CO_2 Reduction

Electrocatalytic CO_2RR includes three steps, namely, the chemisorption of CO_2 on the surface of electrocatalysts, the transfer of high-energy electrons and protons between two elements to break C=O bonds, and the desorption of products from the surface of the electrocatalysts [57]. For the hybrid system composed of single-atom metals and 2D MoS_2, CO_2RR more frequently occurred on metal, and the reaction paths or products are strongly dependent on the components of metal. These reaction products or paths include three types: (1) the reduction of CO_2 to CO (e.g., on Au or Ag), (2) the reduction of CO_2 to formic acid (e.g., on Sn and Pb), and (3) the reduction of CO or carbon–oxygen compounds to hydrocarbons or alcohols (e.g., on Cu, Fe, and Mn) (**Table 1**).

Table 1. Summary of various single-atom metals supported at 2D MoS_2 for electrochemical CO_2 reduction.

Catalyst	Potential Determining Steps	Limiting Potentials (V)	Overpotential (V)	Production for Catalysts	Ref.
Fe@MoS_2	$*HCOO \rightarrow *HCOOH$	−0.39	0.56	CH_4	[58]
Co@MoS_2	$*HCOO \rightarrow *HCOOH$	−0.24	0.41	CH_4	[58]
Ni@MoS_2	$CO_2 \rightarrow *HCOO$	−0.45	0.62	CH_4	[58]
Cu@MoS_2	$*OCH_3 \rightarrow CH_4 + *O$	−1.05	1.22	CH_4	[58]
Ru@MoS_2	$*CO \rightarrow *CHO$	−0.73	0.9	CH_4	[59]
Pd@MoS_2	$CO_2 \rightarrow *HCOO$	−0.96	1.13	CH_4	[60]
Pt@MoS_2	$CO_2 \rightarrow *HCOO$	−0.50	0.67	CH_4	[60]

3.2. Electrochemical Water Splitting

In a conventional water electrolyzer, HER reaction occurs at the cathode and H_2 is separated out, while OER reaction occurs at the anode and O_2 is separated out (**Figure 2**a) [61][62][63]. Under standard conditions, a thermodynamic potential of 1.23 V is required to drive electrochemical water splitting (**Figure 2**b) for HER and OER. However, in real conditions, the input potential of water splitting in practical electrolyzers is much larger than 1.23 V. In general, a high-performance electrocatalyst for water splitting is still focused on noble-metal-based catalysts (e.g., Pt for HER and IrO_2 or RuO_2 for OER) (**Table 2**); however, it is necessary to develop noble metal-free electrocatalysts or decrease the loading amount of noble metals electrocatalysts because of the prohibitive cost and scarce reserve. For the reaction mechanisms (e.g., the Volmer–Heyrovsky mechanism) or paths for HER used in calculation models, there are three elementary steps regarding interactions between the water dissociates and a reactive hydrogen intermediate (absorbed hydrogen on the catalyst surface, H_{ad}), including the Volmer step followed by either the Heyrovsky step ($H_2O + H_{ad} + e^- \leftrightarrow H_2 + OH^-$) or the Tafel recombination step ($2H_{ad} \leftrightarrow H_2$). The detailed mechanism or reaction path is dependent on the components of metal.

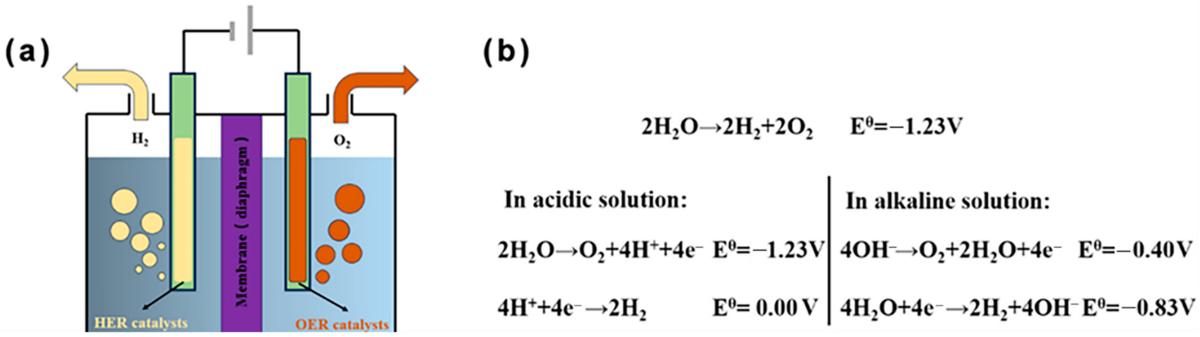

Figure 2. (**a**) Illustration of conventional water electrolyzers. (**b**) Water-splitting reactions under acidic and alkaline conditions.

Table 2. Summary of typical single-atom metal/2D MoS_2 hybrid nanomaterials for water splitting.

Catalyst	Electrolyte	η (mV)/Best Ratio (w.t.% or Concentration)	Tafel Slope (mV dec $^{-1}$)	Stability Test	Ref.
Co/2D MoS_2	0.5 M H_2SO_4	42/3.5% Co/1T-MoS_2	32	10,000 CVs	[64]
Pt/2D MoS_2	0.1 M H_2SO_4	60/1.5% Pt/MoS_2	96	5000 CVs	[20]
Pd/2D MoS_2	0.5 M H_2SO_4	89/1% Pd/1T-MoS_2	62	5000 CVs	[65]
Ni/2D MoS_2	0.5 M H_2SO_4	98/Ni/MoS_2	103	2000 CVs	[66]
Ru/2D MoS_2	0.5 M H_2SO_4	114/46 μg cm^{-2} Ru/MoS_2	-	10 h	[67]

Catalyst	Electrolyte	η (mV)/Best Ratio (w.t.% or Concentration)	Tafel Slope (mV dec $^{-1}$)	Stability Test	Ref.
Cu/2D MoS_2	0.5 M H_2SO_4	131/1% Cu/MoS_2	51	7 h	[54]
Fe, Co, Ni, Pd, Pt/2D MoS_2	0.5 M H_2SO_4	140/2.7% Pd/1T-MoS_2	57	1000 CVs	[68]
Ni/2D MoS_2	0.5 M H_2SO_4	174/1% Ni/MoS_2	69	1000 CVs	[69]
Au, Pt, Pd/2D MoS_2	0.5 M H_2SO_4	210/1.1% Pt/MoS_2	104	5 h	[70]
Ni/2D MoS_2	0.5 M H_2SO_4	263/2.7% Ni/MoS_2	81	1000 CVs	[71]
Ru/2D MoS_2	1.0 M PBS	125/46 μg cm^{-2} Ru/MoS_2	-	10 h	[67]
Ru/2D MoS_2	1.0 M KOH	41/46 μg cm^{-2} Ru/MoS_2	114	20 h	[67]
Ir/2D MoS_2	1.0 M KOH	44/Ir/1T-MoS_2	32	9000 CVs	[72]
Ni/2D MoS_2	1.0 M KOH	110/Ni/MoS_2	119	2000 CVs	[66]

Note: overpotential value (η) and stability test were performed at the current density of 10 mA cm^{-2}; CVs, cycles.

References

1. Chen, Y.; Ji, S.; Chen, C.; Peng, Q.; Wang, D.; Li, Y. Single-atom catalysts: Synthetic strategies and electrochemical applications. Joule 2018, 2, 1242–1264.
2. Zhang, J.; Zhao, Y.; Guo, X.; Chen, C.; Dong, C.-L.; Liu, R.-S.; Han, C.-P.; Li, Y.; Gogotsi, Y.; Wang, G. Single platinum atoms immobilized on an MXene as an efficient catalyst for the hydrogen evolution reaction. Nat. Catal. 2018, 1, 985–992.
3. Gu, J.; Hsu, C.-S.; Bai, L.; Chen, H.M.; Hu, X. Atomically dispersed Fe3+ sites catalyze efficient CO2 electroreduction to CO. Science 2019, 364, 1091–1094.
4. Wang, A.; Li, J.; Zhang, T. Heterogeneous single-atom catalysis. Nat. Rev. Chem. 2018, 2, 65–81.

5. Khan, I.; Yuan, A.; Khan, S.; Khan, A.; Khan, S.; Shah, S.A.; Luo, M.; Yaseen, W.; Shen, X.; Yaseen, M. Graphitic carbon nitride composites with gold and ZIF-67 nanoparticles as visible-light-promoted catalysts for CO2 conversion and bisphenol A degradation. ACS Appl. Nano Mater. 2022, 5, 13404–13416.
6. Khan, I.; Kang, K.; Khan, A.; Jiyuan, G.; Khan, S.; Khan, S.; Basir, A.; Sadiq, S. Efficient CO2 conversion and organic pollutants degradation over Sm3+ doped and rutile TiO2 nanorods decorated-GdFeO3 nanorods. Int. J. Hydrogen Energy 2023, in press.
7. Khan, I.; Luo, M.; Khan, S.; Asghar, H.; Saeed, M.; Khan, S.; Khan, A.; Humayun, M.; Guo, L.; Shi, B. Green synthesis of SrO bridged LaFeO3/g-C3N4 nanocomposites for CO2 conversion and bisphenol A degradation with new insights into mechanism. Environ. Res. 2022, 207, 112650.
8. Liu, H.; Grasseschi, D.; Dodda, A.; Fujisawa, K.; Olson, D.; Kahn, E.; Zhang, F.; Zhang, T.; Lei, Y.; Branco, R.B.N. Spontaneous chemical functionalization via coordination of Au single atoms on monolayer MoS2. Sci. Adv. 2020, 6, eabc9308.
9. Shan, J.; Ye, C.; Jiang, Y.; Jaroniec, M.; Zheng, Y.; Qiao, S.-Z. Metal-metal interactions in correlated single-atom catalysts. Sci. Adv. 2022, 8, eabo0762.
10. Xu, J.; Lai, S.; Qi, D.; Hu, M.; Peng, X.; Liu, Y.; Liu, W.; Hu, G.; Xu, H.; Li, F. Atomic Fe-Zn dual-metal sites for high-efficiency pH-universal oxygen reduction catalysis. Nano Res. 2021, 14, 1374–1381.
11. Zhang, N.; Zhang, X.; Tao, L.; Jiang, P.; Ye, C.; Lin, R.; Huang, Z.; Li, A.; Pang, D.; Yan, H. Silver single-atom catalyst for efficient electrochemical CO2 reduction synthesized from thermal transformation and surface reconstruction. Angew. Chem. Int. Ed. 2021, 60, 6170–6176.
12. Gan, X.; Lei, D.; Ye, R.; Zhao, H.; Wong, K.-Y. Transition metal dichalcogenide-based mixed-dimensional heterostructures for visible-light-driven photocatalysis: Dimensionality and interface engineering. Nano Res. 2021, 14, 2003–2022.
13. Qiao, B.; Wang, A.; Yang, X.; Allard, L.F.; Jiang, Z.; Cui, Y.; Liu, J.; Li, J.; Zhang, T. Single-atom catalysis of CO oxidation using Pt1/FeOx. Nat. Chem. 2011, 3, 634–641.
14. Yang, X.-F.; Wang, A.; Qiao, B.; Li, J.; Liu, J.; Zhang, T. Single-atom catalysts: A new frontier in heterogeneous catalysis. Acc. Chem. Res. 2013, 46, 1740–1748.
15. Jones, J.; Xiong, H.; DeLaRiva, A.T.; Peterson, E.J.; Pham, H.; Challa, S.R.; Qi, G.; Oh, S.; Wiebenga, M.H.; Pereira Hernández, X.I. Thermally stable single-atom platinum-on-ceria catalysts via atom trapping. Science 2016, 353, 150–154.
16. Sun, J.-F.; Wu, J.-T.; Xu, Q.-Q.; Zhou, D.; Yin, J.-Z. CO2 electrochemical reduction using single-atom catalysts. Preparation, characterization and anchoring strategies: A review. Environ. Chem. Lett. 2020, 18, 1593–1623.

17. Kwon, K.C.; Suh, J.M.; Varma, R.S.; Shokouhimehr, M.; Jang, H.W. Electrocatalytic water splitting and CO2 reduction: Sustainable solutions via single-atom catalysts supported on 2D materials. Small Methods 2019, 3, 1800492.
18. Lee, W.H.; Ko, Y.-J.; Kim, J.-Y.; Min, B.K.; Hwang, Y.J.; Oh, H.-S. Single-atom catalysts for the oxygen evolution reaction: Recent developments and future perspectives. Chem. Commun. 2020, 56, 12687–12697.
19. Li, X.; Cui, P.; Zhong, W.; Li, J.; Wang, X.; Wang, Z.; Jiang, J. Graphitic carbon nitride supported single-atom catalysts for efficient oxygen evolution reaction. Chem. Commun. 2016, 52, 13233–13236.
20. Deng, J.; Li, H.; Xiao, J.; Tu, Y.; Deng, D.; Yang, H.; Tian, H.; Li, J.; Ren, P.; Bao, X. Triggering the electrocatalytic hydrogen evolution activity of the inert two-dimensional MoS2 surface via single-atom metal doping. Energy Environ. Sci. 2015, 8, 1594–1601.
21. He, T.; Zhang, C.; Du, A. Single-atom supported on graphene grain boundary as an efficient electrocatalyst for hydrogen evolution reaction. Chem. Eng. Sci. 2019, 194, 58–63.
22. Vancsó, P.; Popov, Z.I.; Pető, J.n.; Ollár, T.; Dobrik, G.; Pap, J.z.S.; Hwang, C.; Sorokin, P.B.; Tapasztó, L. Transition metal chalcogenide single layers as an active platform for single-atom catalysis. ACS Energy Lett. 2019, 4, 1947–1953.
23. Zhou, X.; Li, K.; Lin, Y.; Song, L.; Liu, J.; Liu, Y.; Zhang, L.; Wu, Z.; Song, S.; Li, J. A single-atom manipulation approach for synthesis of atomically mixed nanoalloys as efficient catalysts. Angew. Chem. 2020, 132, 13670–13676.
24. Su, H.; Zhou, W.; Zhang, H.; Zhou, W.; Zhao, X.; Li, Y.; Liu, M.; Cheng, W.; Liu, Q. Dynamic evolution of solid–liquid electrochemical interfaces over single-atom active sites. J. Am. Chem. Soc. 2020, 142, 12306–12313.
25. Zhang, X.; Guo, J.; Guan, P.; Liu, C.; Huang, H.; Xue, F.; Dong, X.; Pennycook, S.J.; Chisholm, M.F. Catalytically active single-atom niobium in graphitic layers. Nat. Commun. 2013, 4, 1924.
26. Gan, X.; Zhang, J.; Liu, J.; Bai, Y.; Su, X.; Wang, W.; Cao, Z.; Zhao, H.; Ao, Y.; Wang, P. Polyaniline Functionalization of Defective 1T-MoS2 Nanosheets for Improved Electron and Mass Transfer: Implications for Electrochemical Sensors. ACS Appl. Nano Mater. 2023, 6, 11725–11736.
27. Hou, C.C.; Zou, L.; Sun, L.; Zhang, K.; Liu, Z.; Li, Y.; Li, C.; Zou, R.; Yu, J.; Xu, Q. Single-atom iron catalysts on overhang-eave carbon cages for high-performance oxygen reduction reaction. Angew. Chem. 2020, 132, 7454–7459.
28. Zhu, J.; Cai, L.; Yin, X.; Wang, Z.; Zhang, L.; Ma, H.; Ke, Y.; Du, Y.; Xi, S.; Wee, A.T. Enhanced electrocatalytic hydrogen evolution activity in single-atom Pt-decorated VS2 nanosheets. ACS Nano 2020, 14, 5600–5608.

29. Rao, R.G.; Blume, R.; Hansen, T.W.; Fuentes, E.; Dreyer, K.; Moldovan, S.; Ersen, O.; Hibbitts, D.D.; Chabal, Y.J.; Schlögl, R. Interfacial charge distributions in carbon-supported palladium catalysts. Nat. Commun. 2017, 8, 340.

30. Gan, X.; Zhao, H.; Quan, X. Two-dimensional MoS2: A promising building block for biosensors. Biosens. Bioelectron. 2017, 89, 56–71.

31. Liu, T.; Zhao, X.; Liu, X.; Xiao, W.; Luo, Z.; Wang, W.; Zhang, Y.; Liu, J.-C. Understanding the hydrogen evolution reaction activity of doped single-atom catalysts on two-dimensional GaPS4 by DFT and machine learning. J. Energy Chem. 2023, 81, 93–100.

32. Xiao, Z.; Gan, X.; Zhu, T.; Lei, D.; Zhao, H.; Wang, P. Activating the Basal Planes in 2H-MoTe2 Monolayers by Incorporating Single-Atom Dispersed N or P for Enhanced Electrocatalytic Overall Water Splitting. Adv. Sustain. Syst. 2022, 6, 2100515.

33. Gan, X.; Lei, D.; Wong, K.-Y. Two-dimensional layered nanomaterials for visible-light-driven photocatalytic water splitting. Mater. Today Energy 2018, 10, 352–367.

34. Pan, U.N.; Paudel, D.R.; Das, A.K.; Singh, T.I.; Kim, N.H.; Lee, J.H. Ni-nanoclusters hybridized 1T–Mn–VTe2 mesoporous nanosheets for ultra-low potential water splitting. Appl. Catal. B Environ. 2022, 301, 120780.

35. Ertl, G.; Knözinger, H.; Weitkamp, J. Handbook of Heterogeneous Catalysis; VCH: Weinheim, Germany, 1997; Volume 2.

36. Yang, J.; Mohmad, A.R.; Wang, Y.; Fullon, R.; Song, X.; Zhao, F.; Bozkurt, I.; Augustin, M.; Santos, E.J.; Shin, H.S. Ultrahigh-current-density niobium disulfide catalysts for hydrogen evolution. Nat. Mater. 2019, 18, 1309–1314.

37. Gusmão, R.; Veselý, M.; Sofer, Z.k. Recent developments on the single atom supported at 2D materials beyond graphene as catalysts. ACS Catal. 2020, 10, 9634–9648.

38. Shi, Y.; Zhou, Y.; Yang, D.-R.; Xu, W.-X.; Wang, C.; Wang, F.-B.; Xu, J.-J.; Xia, X.-H.; Chen, H.-Y. Energy level engineering of MoS2 by transition-metal doping for accelerating hydrogen evolution reaction. J. Am. Chem. Soc. 2017, 139, 15479–15485.

39. Asadi, M.; Kim, K.; Liu, C.; Addepalli, A.V.; Abbasi, P.; Yasaei, P.; Phillips, P.; Behranginia, A.; Cerrato, J.M.; Haasch, R. Nanostructured transition metal dichalcogenide electrocatalysts for CO2 reduction in ionic liquid. Science 2016, 353, 467–470.

40. Gan, X.; Lee, L.Y.S.; Wong, K.-y.; Lo, T.W.; Ho, K.H.; Lei, D.Y.; Zhao, H. 2H/1T phase transition of multilayer MoS2 by electrochemical incorporation of S vacancies. ACS Appl. Energy Mater. 2018, 1, 4754–4765.

41. Gan, X.; Zhao, H.; Lei, D.; Wang, P. Improving electrocatalytic activity of 2H-MoS2 nanosheets obtained by liquid phase exfoliation: Covalent surface modification versus interlayer interaction. J.

Catal. 2020, 391, 424–434.

42. Zhang, J.; Wang, T.; Pohl, D.; Rellinghaus, B.; Dong, R.; Liu, S.; Zhuang, X.; Feng, X. Interface engineering of MoS2/Ni3S2 heterostructures for highly enhanced electrochemical overall-water-splitting activity. Angew. Chem. 2016, 128, 6814–6819.
43. Linghu, Y.; Tong, T.; Li, C.; Wu, C. The catalytic mechanism of CO2 electrochemical reduction over transition metal-modified 1T'-MoS2 monolayers. Appl. Surf. Sci. 2022, 590, 153001.
44. Ji, S.; Chen, Y.; Wang, X.; Zhang, Z.; Wang, D.; Li, Y. Chemical synthesis of single atomic site catalysts. Chem. Rev. 2020, 120, 11900–11955.
45. Cheng, N.; Stambula, S.; Wang, D.; Banis, M.N.; Liu, J.; Riese, A.; Xiao, B.; Li, R.; Sham, T.-K.; Liu, L.-M. Platinum single-atom and cluster catalysis of the hydrogen evolution reaction. Nat. Commun. 2016, 7, 13638.
46. Lu, Y.; Kuo, C.-T.; Kovarik, L.; Hoffman, A.S.; Boubnov, A.; Driscoll, D.M.; Morris, J.R.; Bare, S.R.; Karim, A.M. A versatile approach for quantification of surface site fractions using reaction kinetics: The case of CO oxidation on supported Ir single atoms and nanoparticles. J. Catal. 2019, 378, 121–130.
47. Repp, J.; Moresco, F.; Meyer, G.; Rieder, K.-H.; Hyldgaard, P.; Persson, M. Substrate mediated long-range oscillatory interaction between adatoms: Cu/Cu(111). Phys. Rev. Lett. 2000, 85, 2981.
48. Ji, Q.; Zhang, Y.; Zhang, Y.; Liu, Z. Chemical vapour deposition of group-VIB metal dichalcogenide monolayers: Engineered substrates from amorphous to single crystalline. Chem. Soc. Rev. 2015, 44, 2587–2602.
49. Xiong, Q.; Zhang, X.; Wang, H.; Liu, G.; Wang, G.; Zhang, H.; Zhao, H. One-step synthesis of cobalt-doped MoS2 nanosheets as bifunctional electrocatalysts for overall water splitting under both acidic and alkaline conditions. Chem. Commun. 2018, 54, 3859–3862.
50. Zhang, F.; Momeni, K.; AlSaud, M.A.; Azizi, A.; Hainey, M.F.; Redwing, J.M.; Chen, L.-Q.; Alem, N. Controlled synthesis of 2D transition metal dichalcogenides: From vertical to planar MoS2. 2D Mater. 2017, 4, 025029.
51. Zhang, H. Ultrathin two-dimensional nanomaterials. ACS Nano 2015, 9, 9451–9469.
52. Li, J.; Chen, S.; Quan, F.; Zhan, G.; Jia, F.; Ai, Z.; Zhang, L. Accelerated dinitrogen electroreduction to ammonia via interfacial polarization triggered by single-atom protrusions. Chem 2020, 6, 885–901.
53. Zeng, Z.; Yin, Z.; Huang, X.; Li, H.; He, Q.; Lu, G.; Boey, F.; Zhang, H. Single-layer semiconducting nanosheets: High-yield preparation and device fabrication. Angew. Chem. 2011, 123, 11289–11293.

54. Ji, L.; Yan, P.; Zhu, C.; Ma, C.; Wu, W.; Wei, C.; Shen, Y.; Chu, S.; Wang, J.; Du, Y. One-pot synthesis of porous 1T-phase MoS2 integrated with single-atom Cu doping for enhancing electrocatalytic hydrogen evolution reaction. Appl. Catal. B Environ. 2019, 251, 87–93.
55. Wang, G.; Zhang, G.; Ke, X.; Chen, X.; Chen, X.; Wang, Y.; Huang, G.; Dong, J.; Chu, S.; Sui, M. Direct Synthesis of Stable 1T-MoS2 Doped with Ni Single Atoms for Water Splitting in Alkaline Media. Small 2022, 18, 2107238.
56. Wang, X.; Zhang, Y.; Wu, J.; Zhang, Z.; Liao, Q.; Kang, Z.; Zhang, Y. Single-atom engineering to ignite 2D transition metal dichalcogenide based catalysis: Fundamentals, progress, and beyond. Chem. Rev. 2021, 122, 1273–1348.
57. Wang, Y.; Han, P.; Lv, X.; Zhang, L.; Zheng, G. Defect and interface engineering for aqueous electrocatalytic CO2 reduction. Joule 2018, 2, 2551–2582.
58. Yu, Q. Theoretical studies of non-noble metal single-atom catalyst Ni1/MoS2: Electronic structure and electrocatalytic CO2 reduction. Sci. China Mater. 2022, 66, 1079–1088.
59. Ilyas, T.; Raziq, F.; Ali, S.; Zada, A.; Ilyas, N.; Shaha, R.; Wang, Y.; Qiao, L. Facile synthesis of MoS2/Cu as trifunctional catalyst for electrochemical overall water splitting and photocatalytic CO2 conversion. Mater. Des. 2021, 204, 109674.
60. Ren, Y.; Sun, X.; Qi, K.; Zhao, Z. Single atom supported on MoS2 as efficient electrocatalysts for the CO2 reduction reaction: A DFT study. Appl. Surf. Sci. 2022, 602, 154211.
61. Wang, X.; Zheng, Y.; Sheng, W.; Xu, Z.J.; Jaroniec, M.; Qiao, S.-Z. Strategies for design of electrocatalysts for hydrogen evolution under alkaline conditions. Mater. Today 2020, 36, 125–138.
62. Zhu, J.; Hu, L.; Zhao, P.; Lee, L.Y.S.; Wong, K.-Y. Recent advances in electrocatalytic hydrogen evolution using nanoparticles. Chem. Rev. 2019, 120, 851–918.
63. Pham, V.P.; Yeom, G.Y. Recent advances in doping of molybdenum disulfide: Industrial applications and future prospects. Adv. Mater. 2016, 28, 9024–9059.
64. Qi, K.; Cui, X.; Gu, L.; Yu, S.; Fan, X.; Luo, M.; Xu, S.; Li, N.; Zheng, L.; Zhang, Q. Single-atom cobalt array bound to distorted 1T MoS2 with ensemble effect for hydrogen evolution catalysis. Nat. Commun. 2019, 10, 5231.
65. Luo, Z.; Ouyang, Y.; Zhang, H.; Xiao, M.; Ge, J.; Jiang, Z.; Wang, J.; Tang, D.; Cao, X.; Liu, C. Chemically activating MoS2 via spontaneous atomic palladium interfacial doping towards efficient hydrogen evolution. Nat. Commun. 2018, 9, 2120.
66. Wang, Q.; Zhao, Z.L.; Dong, S.; He, D.; Lawrence, M.J.; Han, S.; Cai, C.; Xiang, S.; Rodriguez, P.; Xiang, B. Design of active nickel single-atom decorated MoS2 as a pH-universal catalyst for hydrogen evolution reaction. Nano Energy 2018, 53, 458–467.

67. Wang, D.; Li, Q.; Han, C.; Xing, Z.; Yang, X. Single-atom ruthenium based catalyst for enhanced hydrogen evolution. Appl. Catal. B Environ. 2019, 249, 91–97.
68. Lau, T.H.; Wu, S.; Kato, R.; Wu, T.-S.; Kulhavy, J.; Mo, J.; Zheng, J.; Foord, J.S.; Soo, Y.-L.; Suenaga, K. Engineering monolayer 1T-MoS2 into a bifunctional electrocatalyst via sonochemical doping of isolated transition metal atoms. ACS Catal. 2019, 9, 7527–7534.
69. Luo, R.; Luo, M.; Wang, Z.; Liu, P.; Song, S.; Wang, X.; Chen, M. The atomic origin of nickel-doping-induced catalytic enhancement in MoS2 for electrochemical hydrogen production. Nanoscale 2019, 11, 7123–7128.
70. Xuan, N.; Chen, J.; Shi, J.; Yue, Y.; Zhuang, P.; Ba, K.; Sun, Y.; Shen, J.; Liu, Y.; Ge, B. Single-atom electroplating on two dimensional materials. Chem. Mater. 2018, 31, 429–435.
71. Zhang, H.; Yu, L.; Chen, T.; Zhou, W.; Lou, X.W. Surface modulation of hierarchical MoS2 nanosheets by Ni single atoms for enhanced electrocatalytic hydrogen evolution. Adv. Funct. Mater. 2018, 28, 1807086.
72. Wei, S.; Cui, X.; Xu, Y.; Shang, B.; Zhang, Q.; Gu, L.; Fan, X.; Zheng, L.; Hou, C.; Huang, H. Iridium-triggered phase transition of MoS2 nanosheets boosts overall water splitting in alkaline media. ACS Energy Lett. 2018, 4, 368–374.

Retrieved from https://encyclopedia.pub/entry/history/show/114548